A NASTRAN-BASED COMPUTER PROGRAM FOR STRUCTURAL DYNAMIC ANALYSIS OF HORIZONTAL AXIS WIND TURBINES*

Don W. Lobitz

Sandia National Laboratories
Albuquerque, New Mexico 87185

ABSTRACT

This paper describes a computer program developed for
structural dynamic analysis of horizontal axis wind
turbines (HAWTs). It is based on the finite element
method through its reliance on NASTRAN for the devel-
opment of mass, stiffness, and damping matrices of the
tower and rotor, which are treated in NASTRAN as
separate structures. The tower is modeled in a sta-
tionary frame and the rotor in one rotating at a
constant angular velocity. The two structures are
subsequently joined together (external to NASTRAN)
using a time-dependent transformation consistent with
the hub configuration. Aerodynamic loads are computed
with an established flow model based on strip theory.
Aeroelastic effects are included by incorporating the
local velocity and twisting deformation of the blade
in the load computation. The turbulent nature of the
wind, both in space and time, is modeled by adding in
stochastic wind increments. The resulting equations
of motion are solved in the time domain using the
implicit Newmark-Beta integrator. Preliminary
comparisons with data from the Boeing/NASA MOD2 HAWT
indicate that the code is capable of accurately and
efficiently predicting the response of HAWTs driven by
turbulent winds.

INTRODUCTION

Throughout the history of the DOE-sponsored horizontal
axis wind turbine (HAWT) program efforts have been
undertaken to develop tools for the structural dynamic
analysis of HAWTs. A number of capabilities have
emerged, including natural mode and frequency calcu-
lations with NASTRAN, rigid-rotor aerodynamic load
codes, dynamic flexible-rotor codes fixed in space at
the hub, and full dynamic models of the rotor turning
on the tower.

The NASTRAN mode and frequency analysis is capable of
tracking some of the frequencies as they increase with
increasing rotor speed due to centrifugal stiffening
but is not adequate for those which are sensitive to
other rotating coordinate system effects.

The rigid-rotor codes require the rigid body motion of
the rotor as input and then compute the aerodynamic
loads along a blade as it moves through one revolution
for steady atmospheric conditions. The calculated
loads are integrated to obtain static section loads
and moments at any station. Even with this simple
model, if a reasonable rigid body motion is pre-
scribed, mean loads are predicted with good accuracy.
However, the vibratory flapwise loads are generally,
substantially underpredicted. An example of a rigid-
rotor aerodynamic load code is the PROP software [Ref.
1], developed at Oregon State University.

The flexible-rotor codes use aerodynamic load models
which are similiar to those used in the rigid-rotor
case, but motion of the rotor relative to the hub is
permitted. Thus the motion of the rotor as well as
the applied loads are computed. Through the inter-
dependence of rotor motions and the aerodynamic loads,
this software accounts for aeroelastic effects. With
these codes, as before, the mean response of the rotor
is accurately predicted, but the vibratory response is
underpredicted. Probably the most widely used of
these codes is MOSTAB [Ref. 2], which is a derivative
of a code developed by Paragon Pacific for the dynamic
analysis of helicopters.

The full dynamic models add the interactions between
the tower and the rotor to the flexible-rotor software
described above. Within the confines of small dis-
placement theory, the rotor is modeled in a rotating
frame, the tower in a fixed one, and the two struc-
tures are connected using time-dependent constraints
or forces. Generally a transient integration tech-
nique is used to solve the resulting equations of
motion. Even with the increased level of sophis-
tication, these codes still underpredict the vibratory
response. Two examples are the MOSTAS code [Ref. 3],
which is from the same family as MOSTAB, and DYLOSAT
[Ref. 4], a proprietary code developed by the Boeing
Aerospace Company.

The software described here, named HAWTDYN, is of the
full dynamic model class. Two features which set it
apart from other codes in this class are its use of
NASTRAN for mass, stiffness and damping matrices, and
output processing, and the inclusion of stochastic
wind increments in the aerodynamic load computation.
Time-dependent constraints, which produces time-
varying coefficients in the equations of motion, are
used to connect the rotor to the tower. Aerodynamic
loads are computed using interference factors pre-
dicted by the PROP code [Ref. 1] for a pre-established
rotor orientation. Aeroelastic effects are included by
incorporating the local velocity and twisting defor-
mation of the blade in the load computation. The
stochastic wind increments are computed by the method
outlined in Ref. 5. The resulting equations of motion
are solved in the time domain using the implicit
Newmark-Beta integrator.

Results are presented for a model of the MOD2 wind
turbine which was designed and fabricated by the
Boeing Aerospace Company (BAC). In addition to a fan-
plot, which shows how the natural frequencies of the
turbine vary with operating speed, structural load
time series have been obtained for two stochastic
winds, one with a mean of 20 mph, and the other 27
mph. These time series are reduced and compared with
field measurements. In order to determine the effect
of the tower on the structural response, the model was
modified to fix the rotor hub. With this alteration,
HAWTDYN is consistent with the codes of the flexible-
rotor class except for its inclusion of stochastic

wind effects. Results are also presented for this model.

The following sections contain a description of the mathematical model upon which HAWTDYN is based, the details of the MOD2 finite element model, presentation and discussion of results, and concluding remarks.

HAWTDYN MATHEMATICAL MODEL

Due to its power and versatility in modeling structures, the finite element method has been chosen as a framework for the derivation of the equations of motion for the HAWT. For this derivation, two coordinate systems are employed in order to represent motions throughout the structure as small relative to the appropriate frame. Thus the tower is modeled in a fixed frame and the rotor in one which rotates at the operational speed of the turbine about an axis which is fixed in space. The origins of both coordinate systems are fixed at the initial hub location. For the latter case, rotating frame effects, such as Coriolis and centrifugal forces, must be included. Considering the tower and rotor as separate structures, the equations of motion for each are represented below:

$$M_T \ddot{U}_T + C_T \dot{U}_T + K_T U_T = F_T.$$ (1)

$$M_R \ddot{U}_R + \left(C_R + C_\Omega\right) \dot{U}_R + \left(K_R - S_\Omega\right) U_R = F_c + F_s + F_a.$$

Here the subscripts T and R refer to the tower and rotor respectively. The quantities, C_Ω and S_Ω, which derive from rotating coordinate system effects, are the Coriolis and softening matrices. The softening matrix accounts for changes in the centrifugal force that result from the structural deformations. These matrices are developed in detail in Ref. 6. On the right hand sides of the equations are the applied forces, with the subscripts c, g and a referring to the centrifugal, gravitational and aerodynamic forces, respectively.

These equations can be combined into one matrix equation as follows:

$$\begin{bmatrix} M_T & 0 \\ 0 & M_R \end{bmatrix} \begin{Bmatrix} \ddot{U}_T \\ \ddot{U}_R \end{Bmatrix} + \begin{bmatrix} C_T & 0 \\ 0 & C_R + C_\Omega \end{bmatrix} \begin{Bmatrix} \dot{U}_T \\ \dot{U}_R \end{Bmatrix} + \begin{bmatrix} K_T & 0 \\ 0 & K_R - S_\Omega \end{bmatrix} \begin{Bmatrix} U_T \\ U_R \end{Bmatrix}$$
$$= \begin{Bmatrix} F_T \\ F_c + F_g + F_a \end{Bmatrix}.$$ (2)

Denoting the time-dependent constraint relation which connects the rotor to the tower, consistent with the hub configuration, as Λ, the final set of displacements, velocities and accelerations, U, $\dot{U}$ and $\ddot{U}$, can be derived from,

$$\begin{Bmatrix} U_T \\ U_R \end{Bmatrix} = \Lambda U, \quad \begin{Bmatrix} \dot{U}_T \\ \dot{U}_R \end{Bmatrix} = \dot{\Lambda} U + \Lambda \dot{U},$$
$$\begin{Bmatrix} \ddot{U}_T \\ \ddot{U}_R \end{Bmatrix} = \ddot{\Lambda} U + 2\dot{\Lambda} \dot{U} + \Lambda \ddot{U}.$$ (3)

If the matrices of Eqn. (2) are renamed $\bar{M}$, $\bar{C}$ and $\bar{K}$, and the force vector, $\bar{F}$, the following equation is obtained from the combination of Eqns. (2) and (3), and premultiplication by Λ^T:

$$\left(\Lambda^T \bar{M} \Lambda \right) \ddot{U} + \left(\Lambda^T \bar{C} \Lambda + 2\Lambda^T \bar{M} \dot{\Lambda} \right) \dot{U}$$
$$+ \left(\Lambda^T \bar{K} \Lambda + \Lambda^T \bar{M} \ddot{\Lambda} + \Lambda^T \bar{C} \dot{\Lambda} \right) U = \Lambda^T \bar{F}.$$ (4)

The transformation matrix, Λ, only modifies terms in the matrices associated with tower or rotor connection nodes, and, by judicious selection of the physical modeling at these points, certain terms in Eqn. (4) can be simplified. For example, if the tower connection node possesses only lumped translational mass, the terms, $\Lambda^T \bar{M} \Lambda$, $\Lambda^T \bar{M} \dot{\Lambda}$, and $\Lambda^T \bar{M} \ddot{\Lambda}$, are rendered independent of time and need only be computed once. Moreover, if the tower connection node is not directly involved in any damping, the term $\Lambda^T \bar{C} \Lambda$ also becomes time-independent and $\Lambda^T \bar{C} \dot{\Lambda}$ vanishes. The remaining quantity, $\Lambda^T \bar{K} \Lambda$, will normally be a function of time and must be recomputed at each time step.

Replacing the coefficient matrices of Eqn. (4) by M, C and K, the system equations of motion are obtained and presented below:

$$M\ddot{U} + C\dot{U} + KU = F.$$ (5)

Eqn (5) is complicated by the fact that centrifugal stiffening, which arises due to the spanwise stretching of the blade under the action of the centrifugal loads, must be taken into account. This stretching causes the stiffness to be a function of the deformation [Ref. 6], necessitating more complex solution procedures. To avoid this complexity, the stiffness matrix, K_R, in Eqn. (1) is modified to be commensurate with the quasi-static displacement field associated with the centrifugal loads. This is accomplished through iterative solution of the following equation:

$$\left[K_R \left(U_R \right) \right] \left| U_R \right| = \left[S_\Omega \right] \left| U_R \right| + \left| F_c \right|.$$ (6)

The resulting approximate or mean stiffness matrix represents the rotor stiffness for the operating speed corresponding to the centrifugal loads in Eqn. (6). Thus solutions of Eqn. (5) must be interpreted as motions about a prestressed state.

The aerodynamic forces of Eqn. (1) are computed, taking into account blade velocities and deformations relative to the rotating coordinate system. This provides for the representation of aerodynamic stiffness and damping in the equations of motion. In order to compute these forces, a local blade coordinate system is defined using instantaneous unit chord and span vectors, e_c and e_s, which account for initial blade position and pretwist, and the local blade deformations. The positive senses are from leading to trailing edge for chord, and from hub to tip for the span. The third instantaneous unit direction is identified as the flap vector, e_f, and defined by the cross product of the chord and span vectors. The

relative wind velocity vector, W_r, is given by the following expression:

$$W_r = \left(1-\varepsilon\right) W_m + W_{si} - \left[\dot{U}_R + \Omega \times \left(X_R + U_R\right)\right]. \quad (7)$$

Here, W_m is the mean axial wind, which can include variations due to wind shear and tower shadow; ε is the velocity reduction factor corresponding to a trim solution for the mean wind; W_{si} is the axial stochastic wind increment computed using the methods described in Ref. 5; Ω is the operating speed of the turbine; and, X_R is the initial local position vector. The direction of lift, e_L, is obtained by taking the cross product of W_r and e_s, and then adjusting the sign of the resulting vector so that its dot product with e_c is negative. The direction of drag, e_D, is subsequently computed to be perpendicular to the direction of lift and e_s, this time adjusting the sign so that the dot product of the resulting vector with e_c is positive. With these directions defined, the angle of attack, and the lift and drag forces per unit length are given by,

$$\tan\alpha = -\frac{e_D \cdot e_f}{e_D \cdot e_c},$$

$$L = \frac{1}{2} \rho a W_n^2 C_L(\alpha) e_L, \quad (8)$$

$$D = \frac{1}{2} \rho a W_n^2 C_D(\alpha) e_D.$$

In Eqn. (8), ρ is the air density, a is the length of the chord and C_L and C_D are the coefficients of lift and drag respectively. The quantity, W_n, is the magnitude of the component of the relative wind vector normal to the span vector, computed as follows:

$$W_n = \left|W_r \times e_s\right|. \quad (9)$$

The lift and drag forces are combined with the gravity forces to obtain the total force vector per unit length. This vector is numerically integrated along the length of each blade element, using a Galerkin formulation to obtain concentrated nodal forces.

Time-domain solutions to Eqn. (5) are obtained numerically using an implicit integration technique. For equations with constant coefficients implicit methods are unconditionally stable, which means that the size of the time step is only limited by the desired frequency resolution. The option for larger time steps provides a means to analyze structural response to stochastic loading, which requires long-time solutions. The equations of motion for the HAWT contain time-dependent coefficients, and therefore, unconditional stability is not guaranteed. However, certain "ad hoc" procedures can be implemented which improve the stability and permit reasonably large time steps.

The first implicit scheme implemented, the Hilber-Hughes algorithm [Ref. 7], exhibited unstable growth in the high-frequency response, even though it is advertised to numerically dampen these modes. This may have been caused by the fact that the algorithm is not entirely consistent with the Newton method of equation solution. Experience has indicated that efforts to make the solution procedure conform to this method usually produce a stabilizing effect. For example, the stability of the response was significantly improved by changing the evaluation of the damping term in Eqn. (5) from the beginning to the end of the time step. Because of its conformity to the Newton method, the Newmark-Beta implicit integration scheme [Ref. 8] was the final choice for the solution procedure.

Eqn. (5), discretized in time according to the this algorithm, is presented below:

$$M\ddot{U}_{t+\Delta t} + C\dot{U}_{t+\Delta t} + K_{t+\Delta t} = F_{t+\Delta t},$$
$$U_{t+\Delta t} = U_t + \Delta t \dot{U}_t + \Delta t^2 \left[\left(\frac{1}{2}-\beta\right)\ddot{U}_t + \beta\ddot{U}_{t+\Delta t}\right], \quad (10)$$
$$\dot{U}_{t+\Delta t} = \dot{U}_t + \Delta t \left[(1-\gamma)\ddot{U}_t + \gamma\ddot{U}_{t+\Delta t}\right],$$
$$\beta = .3025, \quad \gamma = .6.$$

The final form of the equation is obtained by making the substitutions indicated in Eqn. (10) and rearranging so that only terms associated with $\ddot{U}_{t+\Delta t}$ appear on the left hand side, as follows:

$$\left[M + \Delta t \gamma C + \Delta t^2 \beta K_{t+\Delta t}\right]\ddot{U}_{t+\Delta t}$$
$$= \left[-\Delta t(1-\gamma)C - \Delta t^2\left(\frac{1}{2}-\beta\right)K_{t+\Delta t}\right]\ddot{U}_t$$
$$+ \left[-C - \Delta t K_{t+\Delta t}\right]\dot{U}_t \quad (11)$$
$$+ \left[K_{t+\Delta t}\right]U_t + F_{t+\Delta t}.$$

Even with the provisions described above to stabilize the solution procedures, a small amount of growth still occurs for some of the HAWT models that have been created. Although the origin of this growth, be it physical or numerical, has not yet been determined, it can be eliminated by the incorporation of structural damping (of the order of 5% of critical).

In order to avoid duplication of such things as development of finite element matrices, solution procedures, and input and output processing, the MacNeal-Schwendler version of NASTRAN was selected as the basis for this development. This particular code was chosen for several reasons. First, NASTRAN is a general purpose finite element code which contains the necessary input options required for producing reasonably accurate models of HAWTs. Solution procedures are available which provide for inclusion of centrifugal stiffening effects in the rotor. The DMAP programming feature of NASTRAN, which allows the user to modify the code without dealing with the FORTRAN coding, proved to be very helpful even though it was not heavily used. The direct matrix input (DMI) option, by which matrices can be modified through the input data deck was also invaluable. And finally, because of NASTRAN's widespread use, familiarity with its BULK DATA input lends a degree of user-friendliness to the present software.
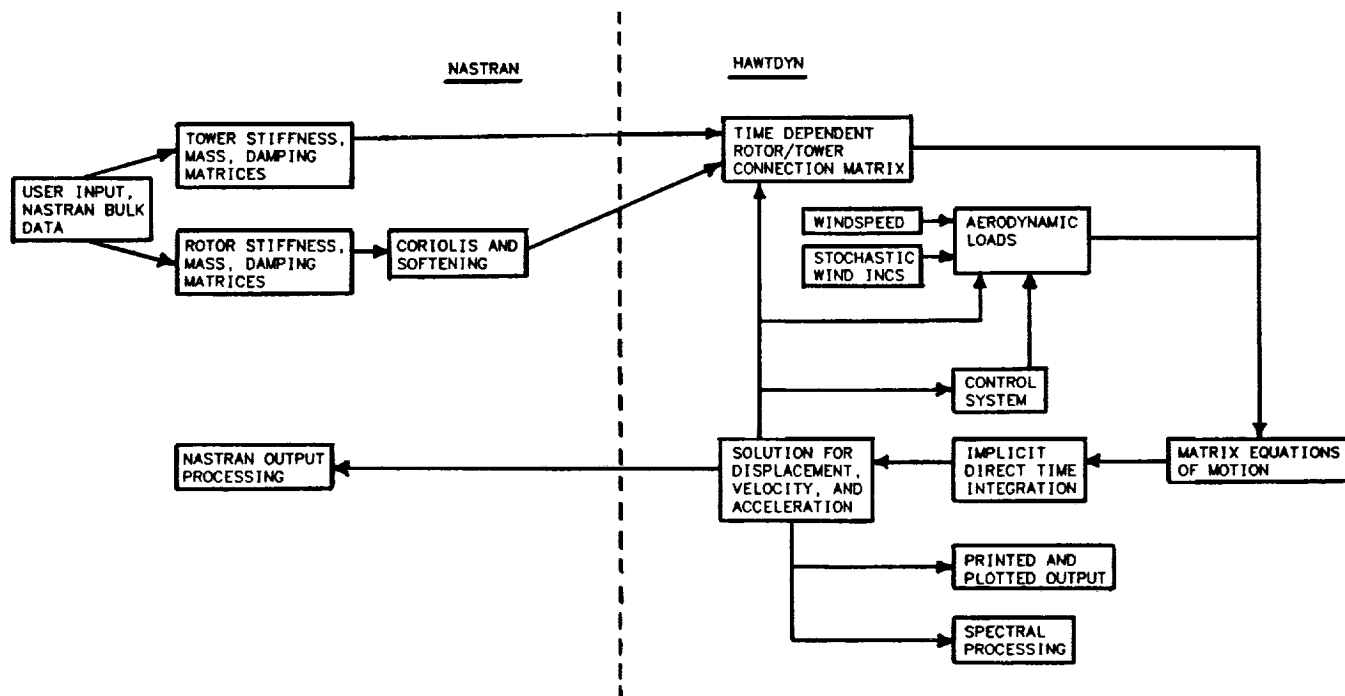
Figure 1. HAWTDYN dynamic analysis method.

The relationships between NASTRAN and HAWTDYN are displayed in the block diagram of Fig. 1. The tower mass, stiffness and damping matrices are developed in NASTRAN relative to a fixed coordinate system. The rotor is modeled in a rotating frame with the stiffness matrix reflecting the effects of centrifugal stiffening. The Coriolis and softening matrices are computed external to NASTRAN and included through the DMI input option. These two sets of matrices are then supplied to HAWTDYN where they are tied together with a rotor/tower connection matrix, which models the particular hub configuration. Aerodynamic loads are obtained using the mean windspeed, the stochastic wind increments, and the local blade motion. Although an active control system has not yet been incorporated into the HAWTDYN software, it would also provide an input to the aerodynamic load computation. The resulting equations of motion are solved using implicit direct time integration. Computed displacement time histories can be printed, plotted, and, in some cases, spectrally analyzed. The NASTRAN code is re-entered for computation of structural loads and stresses.

The PROP code [Ref. 1] has been incorporated into the HAWTDYN software to supply the local free stream wind, interference factors associated with a prescribed orientation of the rotor, and lift and drag coefficients. This relationship is shown in Fig. 2, along with details of the load computation. After the relative wind is obtained using the free stream wind modified by the interference factor, the stochastic wind increments, and the local blade motion, the angle of attack is computed and transmitted to PROP for the determination of the coefficients of lift and drag.
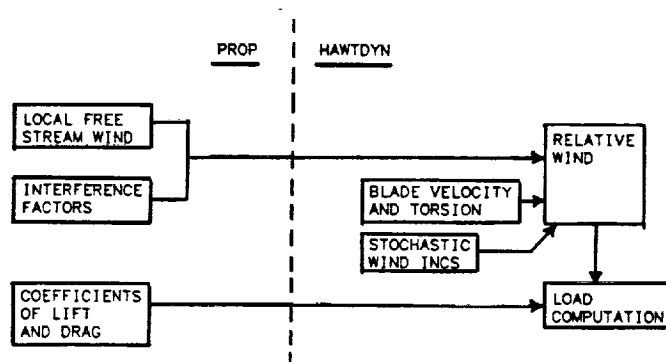

Figure 2. Aerodynamic load computation in HAWTDYN.

DESCRIPTION OF THE MOD2 FINITE ELEMENT MODEL

For an initial test of the performance of HAWTDYN a finite element model of the MOD2 was created. The MOD2 was chosen because of the general interest in that turbine and the availability of experimental data. The model was actually developed using a NASTRAN BULK DATA deck assembled at the Boeing Aerospace Company (BAC) in June of 1981. The BAC model consists of 15 nodes per blade and 14 tower nodes. For HAWTDYN this model was reduced using the NASTRAN ASET option to 5 tower nodes and 5 nodes per blade. This reduced model is shown in Fig. 3. Blade stations 370 and 1164 are indicated in this figure for future reference.
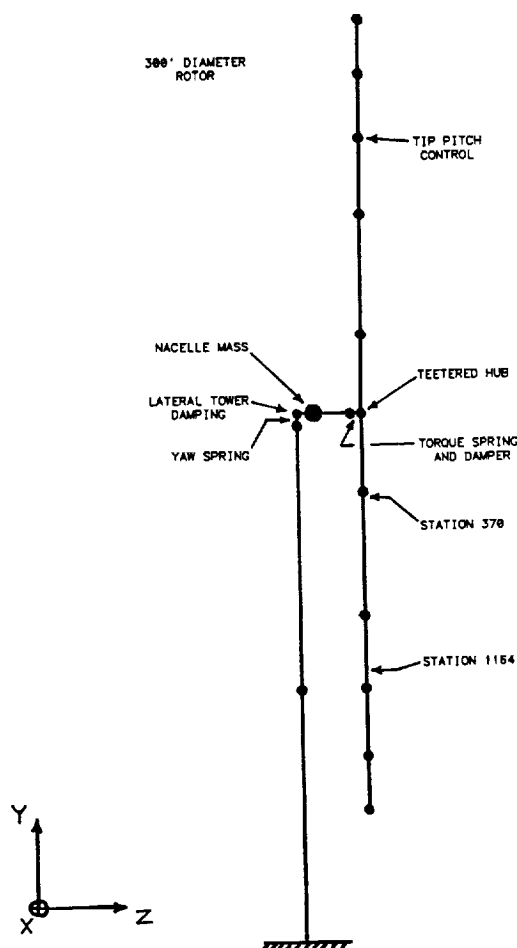
Figure 3. MOD2 finite element model.

The tip pitch control is not modeled in an active sense in HAWTDYN, but rather the tip pitch is preset for use in the aerodynamic load computation. For structural purposes the nominal pitch configuration is used in all cases. The drive train is modeled with a spring and damper attached between the hub and nacelle. The damping in the actual hardware, provided by the tip control, is not included in HAWTDYN, but approximated by setting the drive train damper at 16% of critical. The model includes a yaw spring and lateral tower damping. The values for the tower damping are set at 4% of critical for side-to-side motion, and 1% for fore-aft, consistent with measured results [Ref. 9].

The rotor/tower connection matrix for the MOD2 is shown in Eqn. (12). In this equation, sn represents $\sin(\Omega t)$ and cs, $\cos(\Omega t)$. The upper case XYZ subscripts correspond to the fixed coordinate system, the orientation of which is shown in Fig. 3, and the lower case ones, the rotating frame. Initially, for the blade in the vertical position, these two systems coincide, with the origins of each fixed at the hub. The rotating system turns in a positive sense about the Z axis. The U's and θ's represent displacements along and rotations about the respective axes.

Consistent with the MOD2 hardware, this matrix models a teetered hub. Retained degrees of freedom can be identified by 1's on the diagonal.

$$\left\{\begin{array}{c} U_X \\ U_Y \\ U_Z \\ \theta_X \\ \theta_Y \\ \theta_Z \\ U_x \\ U_y \\ U_z \\ \theta_x \\ \theta_y \\ \theta_z \end{array}\right\}_N = \left[\begin{array}{ccc|ccc|ccc|ccc} & & & & & & cs & -sn & 0 & & & \\ & 0 & & & 0 & & sn & cs & 0 & & 0 & \\ & & & & & & 0 & 0 & 1 & & & \\ \hline & & & 1 & 0 & 0 & & & & & & \\ & 0 & & 0 & 1 & 0 & & 0 & & & 0 & \\ & & & 0 & 0 & 1 & & & & & & \\ \hline & & & & & & 1 & 0 & 0 & & & \\ & 0 & & & 0 & & 0 & 1 & 0 & & 0 & \\ & & & & & & 0 & 0 & 1 & & & \\ \hline & & & 0 & 0 & 0 & & & & 1 & 0 & 0 \\ & 0 & & -sn & cs & 0 & & 0 & & 0 & 0 & 0 \\ & & & 0 & 0 & 0 & & & & 0 & 0 & 1 \end{array}\right] \left\{\begin{array}{c} U_X \\ U_Y \\ U_X \\ \theta_X \\ \theta_Y \\ \theta_Z \\ U_x \\ U_y \\ U_z \\ \theta_x \\ \theta_y \\ \theta_z \end{array}\right\}_O \quad (12)$$

To examine the adequacy of this model, predicted natural frequencies for the rotor parked in the vertical position are compared to measured results taken from Ref. 9. The table below shows frequencies predicted using the original BAC model and the reduced HAWTDYN model, and experimental results for several of the lower frequency modes. These frequencies are normalized by the operating speed of the rotor, which is 17.5 rpm. The column labeled percentage error corresponds to the HAWTDYN model predictions relative to data.

Generally, when experimental data is available, reasonably accurate models can be created by modifying system parameters in a logical fashion such that the errors in the frequency predictions are 5% or less. Most of the errors in Table 1 are of this order. However, for two of the modes, the symmetric flap and the symmetric chord, the errors are particularly high, especially considering their importance in the structural response of the rotor. Although not pursued here, some effort at fine tuning is definitely indicated for a more accurate MOD2 model.

A fanplot for the MOD2 has been constructed by taking fast Fourier transforms on predicted displacement histories associated with the free-vibrations of the turbine. The natural frequencies in this fanplot, which is presented in Fig. 4, are normalized to the operating speed of the rotor (17.5 rpm). This figure demonstrates how the frequencies vary with rpm, and indicates their values at the operating speed. The frequency corresponding to the symmetric flapwise bending mode is of special significance because of its proximity to 4/rev. The nearness of this frequency to that excitation indicates a possibility for larger-than-expected response due to dynamic amplification.

Mode	Freq (/rev) Meas.	Freq (/rev) BAC Model	Freq (/rev) HAWTDYN	% Error
Drive Train	.45	.42	.42	6.6
Tower Fore/Aft	1.23	1.23	1.24	.8
Tower Lateral	1.28	1.25	1.25	2.3
Symmetric Flap	3.30	3.77	3.76	13.9
Symmetric Chord	6.17	6.79	6.69	8.4
Antisym Flap	6.55	7.03	7.03	7.3
Nacelle Pitch	8.23	8.71	8.74	6.2
2nd sym Flap	9.60	10.01	10.01	4.3

HAWTDYN seems to be correctly predicting the response of the rotor to wind shear in that computed displacements indicate a slight turning of the rotor out of the wind about a vertical axis. This motion produces a more uniform relative velocity vector with respect to the angular position of the rotor, and tends to neutralize the effect of wind shear. These results are qualitatively consistent with observed behavior.

For the forced response of the turbine, gravity and wind loading are applied. The wind loads correspond to a wind shear resulting from a surface roughness factor of .25, a value consistent with the MOD2 site at Goodnoe Hills. In addition, the turbulence intensity is set at 20%, also representative of the site. Tower shadow for a width of 15 feet is included through an option in the PROP code. The steady component of the relative wind velocity vector is computed at each Gaussian integration point along the blade (two integration points per element). The stochastic increments are calculated at three stations per blade (stations 874, 1329, and 1655) and linearly interpolated or extrapolated to the Gauss points. Fig. 5 shows the stochastic wind increments for all six stations on the rotor, corresponding to the mean windspeed of 27 mph. At any particular time the width of this band of curves is an indication of the variability of the wind across the rotor.
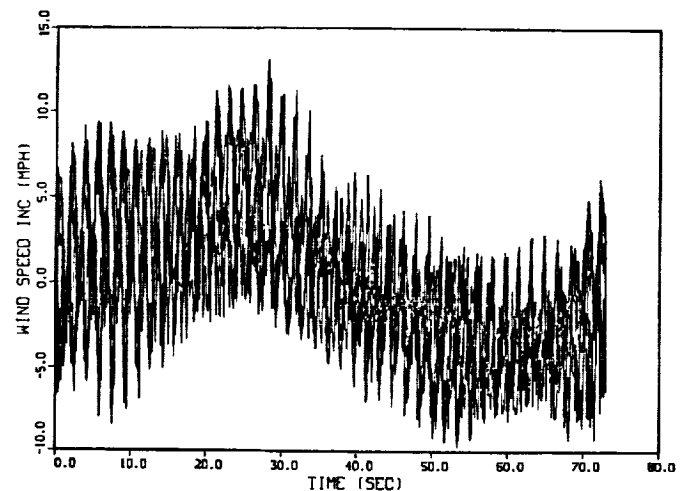

Figure 4. Predicted fanplot for the MOD2.

Figure 5. Stochastic wind increments for a 27 mph mean wind at the six MOD2 rotor stations, three per blade.

PRESENTATION AND DISCUSSION OF RESULTS

In this section to some qualitative observations are discussed, and the predicted response of the MOD2 is presented for windspeeds of 20 and 27 mph. In both cases a turbulent wind increment history is included. For purposes of comparison, results are shown for steady winds at the same windspeeds. Computations are also presented for a configuration of the MOD2 where the hub is fixed in space.

Two qualitative aspects of the results are mentioned here to promote confidence in the HAWTDYN software. First, the aerodynamic damping in the fore-aft direction is definitely present in the solutions and seems to be on the order of 5% of critical. And second,

The predicted edgewise response to this wind at station 370 is presented in Fig. 6. For the first three revolutions on the curve, only gravity and steady wind loads are acting. Thus these three cycles represent the steady response of the turbine. Over the forth cycle the stochastic wind increments are gradually included. The total response of the rotor to all loadings is shown from revolution 5 through 23. For all sections of the curve the response is predominately 1/rev with only slight variations in amplitude. This indicates that the edgewise moments are dominated by the gravity loading, and are not significantly affected by the turbulence in the wind.
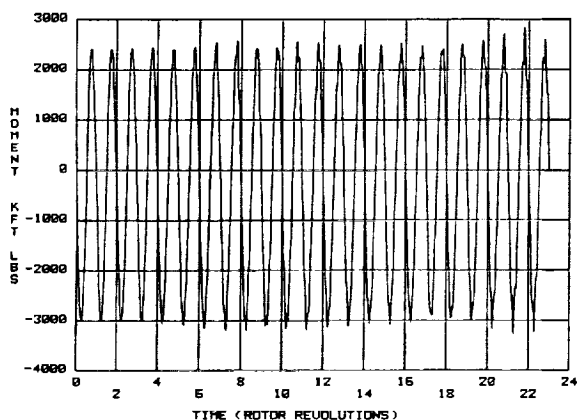
94

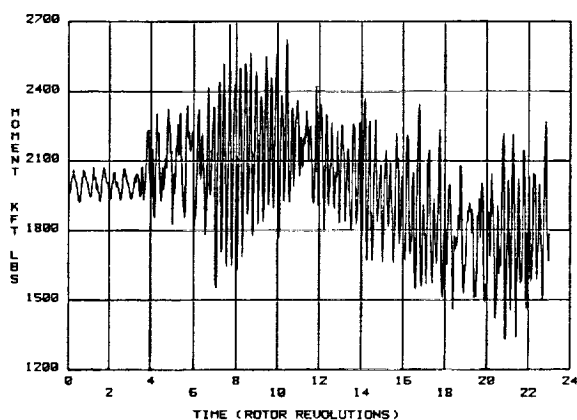Figure 6. Predicted chordwise bending moment for a turbulent wind with a 27 mph mean at station 370 of the MOD2 blade.

Figure 8. Predicted flapwise bending moment filtered using a highpass filter with a cut-off frequency of .25/rev.

The flapwise response at station 370 is shown in Fig. 7. Again the first three cycles represent the steady response and cycles 5 through 23 display the total response. In this case the differences between the steady and total responses are quite dramatic. In addition to a roughly four-fold increase in the cyclic amplitude, the frequency content changes from 2/rev to predominately 4/rev. Thus, for the flapwise moments, the stochastic wind loading dominates the response, in contrast to the edgewise case.

Two additional forms of data reduction are done on the curve of Fig. 8. First it is transformed to determine its frequency content using the fast Fourier transform. The transformed curve, which is shown in Fig. 9, clearly indicates the dominance of the 4/rev component of the response. This dominance is the result of the nearness of the frequency of the symmetric flapwise bending mode to 4/rev at the operating speed. Consistent with the steady wind response, a significant 2/rev component is also present in the total response.

Figure 7. Predicted flapwise bending moment for a turbulent wind with a 27 mph mean at station 370 of the MOD2 blade.

Figure 9. Fast Fourier transform of the filtered flapwise bending moment predictions.

In order to compare with experimental data, the same types of data reduction that are done on the field measurements must be done on the predicted results. To this end, the curve of Fig. 7 is first truncated to delete the first four cycles, filtered with highpass filter to eliminate frequencies below .25/rev and finally truncated again to delete spurious results near the end of the record caused by end-effect problems associated with the filtering. The end product is presented in Fig. 8.
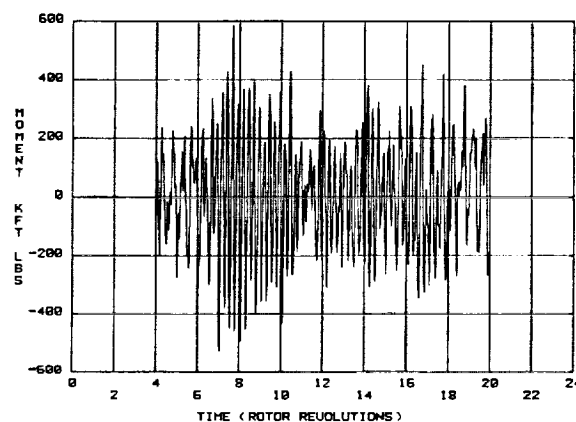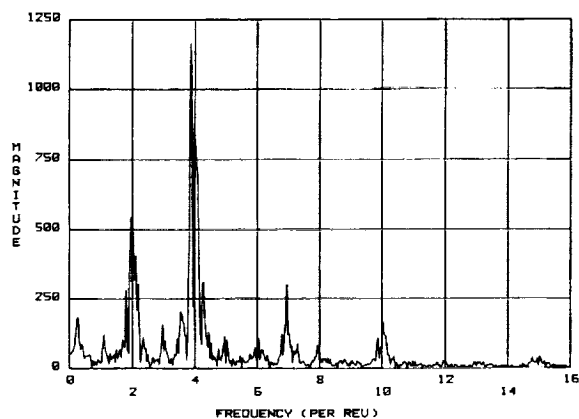
The second form of data reduction consists of cycle counting to obtain a 50 percentile cyclic value. The first step of this procedure involves tabulating all the maximum and minimum values between the zero crossings of Fig. 8. The 50 percentile cyclic value is then obtained by averaging the absolute values of each of the tabulated results.

95

In Fig. 10(b) the 50 percentile cyclic flapwise moment at station 370 is displayed as a function of wind-speed. The experimental data denoted in this figure by the "plus" signs was collected from the MOD2 cluster at Goodnoe Hills in July of 1983. Predictions for two mean windspeeds, 20 and 27 mph, are indicated on the plot by the solid circles. In both cases the predictions fall within the scatter band of the data. The solid triangle corresponds to the predicted value
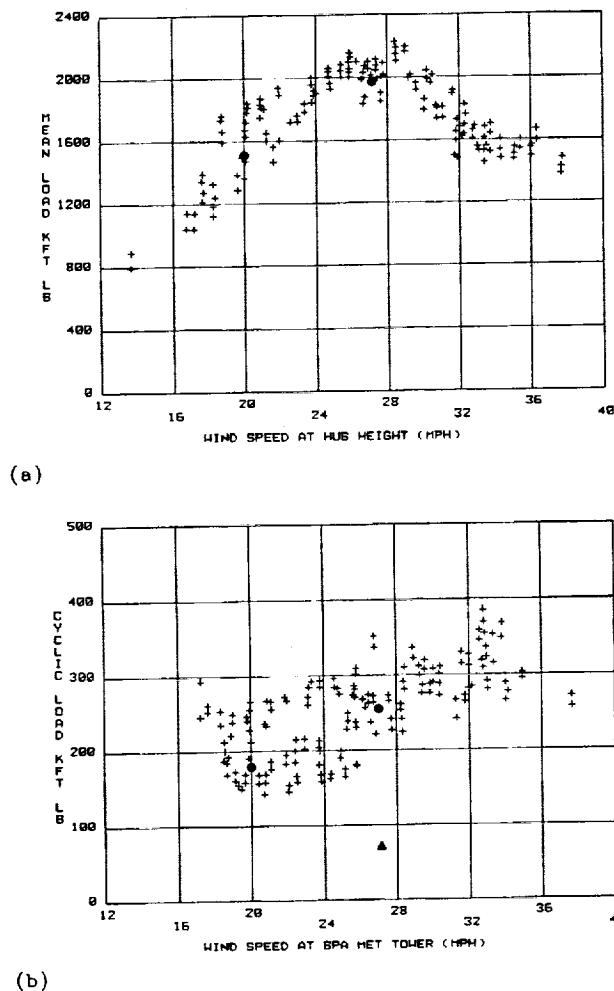

(a)

(b)

Figure 10. Comparison of predictions, denoted by the solid circles and triangle, to data, denoted by the plus signs, at station 370 of the MOD2 blade, (a) mean flapwise bending moment, (b) cyclic flapwise bending moment.

for a steady 27 mph wind. The importance of including turbulent wind effects in the structural dynamic analysis of HAWTs is clearly demonstrated by this figure.

Fig. 10(a) shows the corresponding mean value of the flapwise moment at station 370. As in the cyclic case, the predictions fall within the scatter band of the data. Although not displayed on the plot, the steady wind prediction at 27 mph coincides with the value shown for the total response. This indicates

that the inclusion of stochastic wind effects does not seem to be critical for accurately computing mean flapwise moments.

For station 1164, results similar to those of Fig. 10 are shown in Fig. 11. Again the predictions are generally within the data scatter band, with the mean flapwise moment at the high rim of the band. This slight overprediction is probably caused by the fact that the continuous blade loads are integrated to form concentrated nodal forces. In the static case for a uniform load, this discretization of the load produces moments which are correct at the node points, but overpredicted everywhere in between.
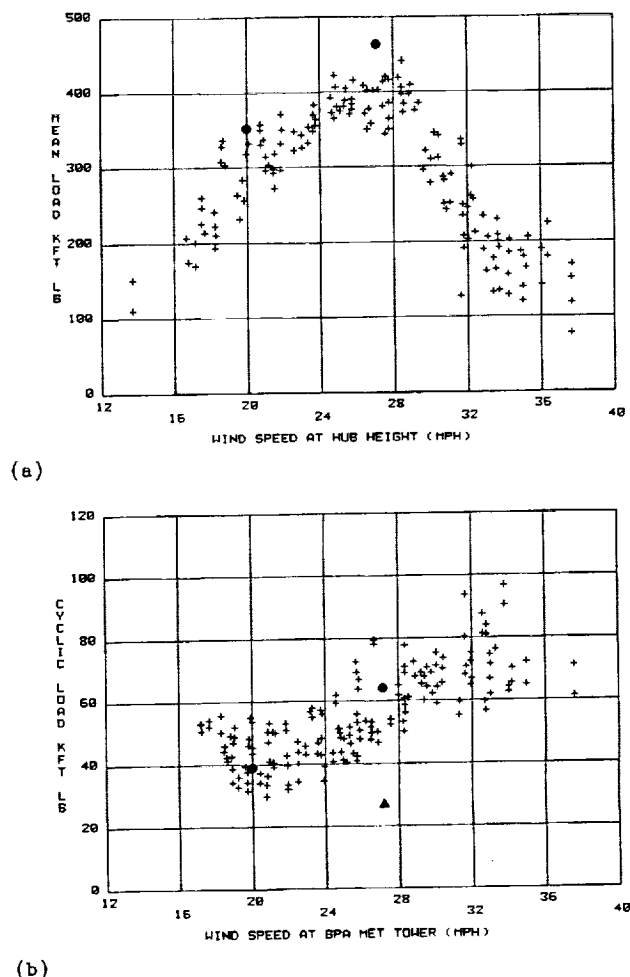

(a)

(b)

Figure 11. Comparison of predictions, denoted by the solid circles and triangle, to data, denoted by the plus signs, at station 1164 of the MOD2 blade, (a) mean flapwise bending moment, (b) cyclic flapwise bending moment.

To examine the role that the tower plays in the response of the MOD2, the hub of the rotor was constrained so that it could not translate. This did not compromise its ability to teeter however. For the same turbulent wind with the 27 mph mean, results show a reduction in the 50 percentile cyclic flapwise moment of approximately 10 percent. Thus, for the

MOD2, it may be possible to eliminate the tower from the analysis without significantly degrading the accuracy of the results. This elimination considerably simplifies the analysis procedures. However, this observation for the MOD2 cannot be generalized to all HAWTs. The critical issue in excluding the tower is the degree to which its presence modifies the natural frequencies of the rotor.

The computer resources required by HAWTDYN are modest. The MOD2 model, which contains 67 degrees of freedom, requires 240 cp seconds on the CRAY computer to obtain solutions out to 80 seconds. The relatively large time step of .008 seconds, made possible by the use of an implicit integration method, was used for these calculations. Although tests were conducted to establish the accuracy of this time step, no attempts were made to find the largest possible time step consistent with accuracy and stability restrictions. Thus, it may be possible to reduce the cp time below the value reported here.

CONCLUSIONS

In the design and analysis of dynamic systems three areas of concern are routinely addressed: the natural frequencies of the system, the excitation frequencies, and the ability of the distributed forces to excite the natural modes. For HAWTs, the task of addressing these areas of concern is not routine. The identification of the natural frequencies of the system is complicated by the fact that the frequencies must be obtained for the turbine in its operational configuration. From the analysis point of view, this entails connecting the rotor, which moves relative to a rotating frame, to the tower which moves relative to a stationary one. This precludes the use of standard solution techniques for obtaining the natural frequencies and modes of the structure. The determination of the excitation frequencies and the spatial distribution of the forces is more involved because of the turbulent nature of the wind. Not only is the turbulence difficult to model, but sophisticated methods for predicting the resultant loads have not been developed. However, with proper attention to creating structural and aerodynamic load models that contain the major physical aspects of the problem, reasonably accurate results can be obtained.

In the present case, the HAWTDYN software has produced accurate predictions for the MOD2 turbine, for two windspeeds. These results are of a preliminary nature and should be viewed as such until more of the validation process has been completed. This process includes making predictions for several existing turbines at a number of wind conditions, and comparing the results with available experimental data. In order to generate more confidence in the present MOD2 finite element model, it should be upgraded so that the computed natural frequencies are in better agreement with measured ones and some development effort should be expended in HAWTDYN to properly model the tip control mechanism.

Even though some aspects of the modeling are crude, HAWTDYN has produced some promising results. The inclusion of turbulent wind effects has dramatically influenced the MOD2 response predictions, bringing them into agreement with measured data. The use of implicit integration methods has posed no insurmountable problems and has made it possible to obtain the long-time solutions required to analyze HAWTs driven by turbulent winds. After the validation process has been completed, it is expected that HAWTDYN will be suitable for accurately evaluating the structural response of alternate HAWT designs.

REFERENCES

1. Patton, E. M., and Wilson, R. E.,"Design Analysis of Performance and Aerodynamic Loading of Non-Flexible Horizontal Axis Wind Turbines," Oregon State University, RLO/2227-78-2, UC-60, August 1978.

2. Dugundji, J., and Wendell, J. H., "General Review of the MOSTAS Computer Code for Wind Turbines," NASA CR-165385, June 1981.

3. Hoffman, J. A.,Dreier, M. E.,Williamson, D. R., and Henninger, W. C., "Mathematical Methods Incorporated in the Wind Energy System Coupled Dynamics Analysis," Paragon Pacific Inc., Report PPI-1014-7, January 1977.

4. DYLOSAT-Proprietary Software Developed by R. D. Miller of the Boeing Aerospace Company, 1983.

5. Veers, P. S., "Modeling Stochastic Wind Loads on Vertical Axis Wind Turbine Blades," Proceedings of the 25th SDM Conference, Palm Springs, May 1978.

6. Weingarten, L. I., and Nickell, R. E., "Non-Linear Stress Analysis of Vertical Axis Wind Turbine Blades," Sandia National Laboratories, SAND74-0378, April 1975.

7. Hilber, H. M., Hughes, T. J. R., and Taylor, R. L., "Improved Numerical Dissipation for Time Integration Algorithms in Structural Dynamics," Earthquake Engineering and Structural Dynamics, Vol.5, pp. 283-292, 1977.

8. Newmark, N. M., "A Method of Computation for Structural Dynamics," Journal of the Engineering Mechanics Division, ASCE, Vol. 85, EM3, pp. 67-94, 1959.

9. Andrews, J. S., and Baskin, J. M., "Development Tests for the 2.5 Megawatt MOD-2 Wind Turbine Generator," Proceedings of the Large Horizontal-Axis Wind Turbines Workshop, NASA Conference Publication 2230, Cleveland, July 1981.